Author Manuscript

Author Manuscript

Author Manuscript

Author Manuscript

HHS Public Access

Author manuscript

Sci Signal. Author manuscript; available in PMC 2023 September 08.

Published in final edited form as:

Sci Signal. 2023 July 25; 16(795): eade5892. doi:10.1126/scisignal.ade5892.

Decreased nitrosylation of CaMKII causes aging-associated impairments in memory and synaptic plasticity in mice†

Nicole L. Rumian[1,2], **Ronald K. Freund**[1], **Mark L. Dell'Acqua**[1,2], **Steven J. Coultrap**[1,*], **K. Ulrich Bayer**[1,2,*]

[1]Department of Pharmacology, University of Colorado Anschutz Medical Campus, Aurora, CO 80045, USA

[2]Program in Neuroscience, University of Colorado Anschutz Medical Campus, Aurora, CO 80045, USA

Abstract

CaMKII has molecular memory functions, because transient Ca^{2+}-stimuli can induce long-lasting increases in its synaptic localization as well as Ca^{2+}-independent (autonomous) activity, thereby leaving memory traces of Ca^{2+}-stimuli beyond their duration. The synaptic effects of two mechanisms that induce CaMKII autonomy are well studied: autophosphorylation at Thr^{286} and binding to GluN2B. Here, we examined the neuronal functions of additional autonomy mechanisms: nitrosylation and oxidation of the CaMKII regulatory domain. We generated a knock-in mouse line with mutations that render the CaMKII regulatory domain nitrosylation/oxidation-incompetent, $CaMKII^{\Delta SNO}$, and found that it had deficits in memory and synaptic plasticity that were similar to those in aged wild-type mice. Also similar to aged wild-type mice, in which CaMKII was hypo-nitrosylated, but unlike mice with impairments of other CaMKII autonomy mechanisms, $CaMKII^{\Delta SNO}$ mice showed reduced long-term potentiation (LTP) when induced by theta-burst stimulation (TBS) but not high-frequency stimulation (HFS). As in aged wildtype mice, the HFS-LTP in the young adult $CaMKII^{\Delta SNO}$ mice required L-type voltage-gated Ca^{2+}-channels. The effects in aged mice were likely caused by the loss of nitrosylation, because no decline in CaMKII oxidation was detected. In hippocampal neurons, nitrosylation of CaMKII induced its accumulation at synapses under basal conditions in a manner mediated by GluN2B binding, like after LTP stimuli. However, LTP-induced synaptic CaMKII accumulation did not require nitrosylation. Thus, an aging-associated decrease in CaMKII nitrosylation may cause impairments by chronic synaptic effects, such as the decrease in basal synaptic CaMKII.

†This manuscript has been accepted for publication in *Science Signaling*. Please refer to the complete, copyedited version on record at https://www.science.org/journal/signaling. The manuscript may not be reproduced or used in any manner that does not fall within the fair use provisions of the Copyright Act without the prior, written permission of AAAS.

*Corresponding author. steve.coultrap@cuanschutz.edu (S.J.C.); ulli.bayer@cuanschutz.edu (K.U.B.).

Author contributions: N.L.R., R.K.F., and S.J.C. performed experiments and analyses; N.L.R., S.J.C., and K.U.B. conceived this study; N.L.R. and K.U.B. wrote the initial draft and all authors contributed to the final manuscript.

Competing interests: K.U.B. is co-founder and board member of Neurexis Therapeutics.

Author Manuscript Author Manuscript Author Manuscript Author Manuscript

INTRODUCTION

Learning and memory is generally thought to require synaptic plasticity, specifically long-term potentiation (LTP)—synaptic strengthening—in the hippocampus. One central mediator of LTP is the Ca^{2+}/calmodulin (CaM)-dependent protein kinase II (CaMKII) (1–3), and LTP requires both CaMKII autophosphorylation within the regulatory domain at Thr^{286} (4) and CaMKII binding to the NMDA-type glutamate receptor subunit GluN2B (5–7). Both Thr^{286} phosphorylation and GluN2B binding have been well-studied, because both generate Ca^{2+}-independent "autonomous" activity of CaMKII, which is regarded as a form of molecular memory (8–10). Additionally, both mechanisms are involved in the persistent synaptic accumulation of CaMKII in response to LTP-stimuli. This accumulation requires direct binding of CaMKII to GluN2B, which can be triggered either by Ca^{2+}/CaM or by phospho-Thr^{286} (9, 11, 12). Even though phospho-Thr^{286} is not strictly required for CaMKII binding to GluN2B (9), it substantially contributes to the stimulus-induced CaMKII binding to GluN2B in cells and to synaptic CaMKII accumulation in hippocampal neurons (12, 13). Alternative mechanisms to induce autonomous CaMKII activity other than by Thr^{286} phosphorylation or by GluN2B binding include oxidation of Met^{281} (14) or simultaneous S-nitrosylation of Cys^{280} and Cys^{289} (15). However, the functional effects of these alternative autonomy mechanisms on the synaptic CaMKII localization or synaptic plasticity has not yet been explored. Whereas protein oxidation has typically been linked to pathological processes, S-nitrosylation can also be induced by physiological signaling with the second messenger nitric oxide (NO) (16, 17). Notably, studies indicate that aging correlates with a general decrease in brain NO and in the S-nitrosylation of neuronal proteins, including CaMKII (18), and aging is well-known to be associated with cognitive decline and selective LTP impairments (19, 20).

In this study, we sought to elucidate the potential roles of CaMKII nitrosylation or oxidation in LTP and learning and memory. To this end, we created a novel mouse line, $CaMKII^{\Delta SNO}$, with nitrosylation/oxidation-incompetent CaMKII mutations of Cys^{280}, Met^{281}, and Cys^{289} to Val residues. We found that these mice had impairments in memory, in LTP, as well as in synaptic CaMKII localization that were similar to those seen here and elsewhere in aged wildtype mice. As aging was found to reduce CaMKII nitrosylation but not oxidation, these results indicate that hypo-nitrosylation directly causes reduction of basal CaMKII localization to synapses, and thereby the synaptic impairments associated with aging.

RESULTS

The cohorts of $CaMKII^{\Delta SNO}$ mutant mice for behavioral analysis

To test the functions of the CaMKIIα regulation by nitrosylation/oxidation at Cys^{280}, Met^{281}, and Cys^{289}, we created a mouse line that prevents this regulation by mutating all three residues to valines: $CaMKII^{C280V/M281V/C289V}$, or $CaMKII^{\Delta SNO}$. This triple mutation affected neither the Ca^{2+}/calmodulin-stimulated activity of CaMKII nor the autonomous CaMKII activity that is induced by Thr^{286} autophosphorylation (fig. S1). $CaMKII^{\Delta SNO}$ mice were analyzed in a battery of behavioral tests. Two age groups were tested: young adult (2 to 3 months old), to test if the $CaMKII^{\Delta SNO}$ mutant is sufficient to induce a phenotype similar as seen with aging; and middle-aged (9 to 12 months old), in case the $CaMKII^{\Delta SNO}$

Author Manuscript Author Manuscript Author Manuscript Author Manuscript

mutant only accelerates age-related impairments in conjunction with modest aging. The size of the young-adult cohorts was determined by power analysis to resolve potential learning and memory deficits both in the radial arm water maze (RAWM) and the contextual fear conditioning (CFC) paradigm. By contrast, the size of the middle-aged cohorts was sufficient to resolve potential differences with confidence only for CFC, but not for RAWM —the test with the higher variability. Additionally, consistent with NIH guidelines, we used and independently analyzed animals of both sexes in all cohorts, though the samples sizes were insufficient to make conclusions about sex-dependent differences.

No indication for impaired anxiety or motor skills in the CaMKII$^{\Delta SNO}$ mutant mice

In the open field test, which assesses for anxiety-like behavior, there was no difference between the genotypes for either age group regarding time spent in either the center or the periphery of the testing chamber; all mice spent more time overall in the periphery (Fig. 1A and fig. S2A). The CaMKII$^{\Delta SNO}$ mice did appear to be more active as they travelled a greater distance, an effect that was observed in both age groups (Fig. 1B and fig. S2B). Similar to this increased locomotor activity in the open field test, rotarod testing indicated enhanced motor coordination, but only in the young adult; in the middle-aged mice, no statistically significant difference was observed (Fig. 1C and fig. S2C). Collectively, performance during these two behavioral tests indicate no impairment of motor skills or changes in anxiety-like behavior in the CaMKII$^{\Delta SNO}$ mice.

The CaMKII$^{\Delta SNO}$ mutation mildly impairs working memory tested in the Y-maze

To assess the role of CaMKII S-nitrosylation in working memory, we subjected our mouse cohorts to the Y-maze test. In this three-armed maze, working memory is tested by examining whether mice correctly alternate arm entries. A correct alternation is when an animal enters each of the three arms without repeating entrance into any one arm; conversely an incorrect alternation is when an animal repeats an arm entry during three turns. In this task, it has been previously shown that older animals have impaired working memory as compared to younger animals (21). Here, the young adult CaMKII$^{\Delta SNO}$ mice had a lower percentage of correct alternations than did young adult wildtype mice (Fig. 1D and fig. S2D), indicating that the CaMKII$^{\Delta SNO}$ mice had a mild impairment in working memory similar, indicated by in arm entries (Fig. 1D and fig. S2D). Among the middle-aged mice, this impairment was smaller and not statistically significant (Fig. 1D and fig. S2D).

The CaMKII$^{\Delta SNO}$ mutation mildly impairs long-term spatial memory in Radial Arm Water Maze

To assess the role of CaMKII S-nitrosylation in long-term spatial memory, we subjected our mouse cohorts to the radial arm water maze (RAWM). In this test, animals are trained to find a hidden platform over two training days and then tested to assess whether they remember the location of that platform during the probe trial, for which the platform has been removed from the maze. This is a typical test to examine both working and long-term spatial memory, and aged animals have previously demonstrated impairments in both in the RAWM (21, 22). Thus, we sought to test whether the CaMKII$^{\Delta SNO}$ mice have any memory impairments in this task. Neither genotype nor age affected ability to learn where the hidden platform was during the two training days, as there were no differences in the latency to

Author Manuscript Author Manuscript Author Manuscript Author Manuscript

reach the platform or in the number of errors in reaching the platform (Fig. 2A,B and fig. S3). The RAWM testing also did not detect any impairment in working memory, even though a working memory impairment was detected in the Y-maze (Fig. 1D). This could be due to the difference in the tests; for instance, the Y-maze simulates free exploration with no escape whereas the RAWM drives an animal to find an escape route as quickly as possible. However, the RAWM probe trial revealed impaired long-term spatial memory in the young adult CaMKII$^{\Delta SNO}$ mice (Fig. 2C), similar as seen previously for aged wildtype mice (21, 22). The impairment manifested as a decrease in the number of times that the young adult CaMKII$^{\Delta SNO}$ entered the goal arm as compared to wildtype. When parsed out by sexes, the impairment was statistically significant only in the male mice; however, our study was not powered to detect differences in the individual sexes and a trend towards impairment was apparent also on the female cohort (Fig. 2C). In the middle-aged group, the impairment did lose statistical significance for both sexes, though likely also because the middle-aged wildtype appeared to perform worse than the young adult wildtype (fig. S3), which again is consistent with aging.

The CaMKII$^{\Delta SNO}$ mutation mildly impairs long-term memory

To assess the role of CaMKII S-nitrosylation in long-term memory, we subjected our mouse cohorts to contextual fear conditioning (CFC). In the testing paradigm used here, the animals were subjected to two foot-shocks on day 1 and returned to the same chamber with no foot-shocks on day 2, with freezing measured across testing (Fig. 3A). CFC is commonly used to determine impairments in long-term memory, and such impairments are seen in older animals (23–25). Thus, we sought to determine if the CaMKII$^{\Delta SNO}$ mice have similar impairments. Indeed, both young adult and middle-aged CaMKII$^{\Delta SNO}$ mice showed significant impairments in the CFC compared to their age-matched wildtype littermates (Fig. 3B,C). However, when the groups were further separated by sex, there was a significant long-term memory impairment in the young adult males but not in the females (fig. S4A,B). By contrast, in the middle-aged group, there was no apparent sex difference (fig. S4C,D).

Overall, the behavioral battery indicates that the CaMKII$^{\Delta SNO}$ have mild impairments in working memory (Y-maze), long-term spatial memory (RAWM), and long-term fear memory (CFC). These mild memory impairments appear to be similar to those previously reported in aged mice and rats (21, 23, 24, 26, 27). By contrast, and as expected, motor impairments seen with aging were not detected in the CaMKII$^{\Delta SNO}$ mice.

The CaMKII$^{\Delta SNO}$ mutation impairs LTP induced by TBS but not HFS

Aged mice are impaired for LTP when induced by mild theta-burst stimulation (TBS) but show normal LTP levels when induced by stronger high-frequency stimulation (HFS) (18, 19). Similar to aged mice, the young adult CaMKII$^{\Delta SNO}$ mice showed impaired LTP when induced by mild TBS (5 episodes of 0.1 Hz, each episode contains 10 stimulus trains of 5 pulses each at 100 Hz) (Fig. 4A and fig. S5A). Also similar to aged mice, but in contrast to other CaMKII autonomy mutants (4, 6), the young adult CaMKII$^{\Delta SNO}$ mice had normal levels of LTP after HFS (specifically 2 trains of 100 Hz pulses, 20 sec apart) (Fig. 4B). Additionally, we tested juvenile CaMKII$^{\Delta SNO}$ mice (13–15 days old), as NMDAR-dependent LTD (induced by 15 min 1 Hz stimulation) is prevalent at this age

Author Manuscript Author Manuscript Author Manuscript Author Manuscript

(28). These juvenile CaMKII$^{\Delta SNO}$ mice had normal levels of LTD, HFS-induced LTP, and subsequent de-potentiation (fig. S5B).

HFS-induced LTP in CaMKII$^{\Delta SNO}$ mice requires both NMDAR and LTCC-mechanisms

Even though aged mice show normal levels of HFS-LTP, it involves different mechanisms than in young animals: In contrast to LTP in younger animals, HFS-LTP in aged mice was not dependent on NMDAR but instead was dependent on L-type voltage-gated Ca^{2+}-channels (LTCCs) (19, 20, 29–33). Thus, we decided to test which mechanism underlies the normal HFS-induced LTP seen in the CaMKII$^{\Delta SNO}$ mice. We found that the HFS-LTP in the CaMKII$^{\Delta SNO}$ mice was still sensitive to pharmacological inhibition of NMDARs (with 50 μM APV) (Fig. 4C). However, similar to aged mice, the HFS-LTP in the CaMKII$^{\Delta SNO}$ mice was now additionally sensitive to inhibition of LTCCs with 10 μM nimodipine (Fig. 4C). By contrast, in young adult wildtype mice, such nimodipine treatment had no effect on HFS-LTP (fig. S5C). Thus, the overall normal levels of HFS-LTP in the young-adult CaMKII$^{\Delta SNO}$ mice appear to require similar compensation mechanisms as seen in aged animals.

The CaMKII nitrosylation directly induces synaptic accumulation through GluN2B binding

It has been suggested that synaptic localization of CaMKII is reduced in aged mice due to the age-related CaMKII hypo-nitrosylation (18). Thus, we decided to test if CaMKII nitrosylation can directly increase synaptic localization. Using an intrabody method, we performed simultaneous live imaging of endogenous CaMKII and markers of either excitatory synapses (PSD-95) or inhibitory synapses (gephyrin) in hippocampal neurons (34, 35). Indeed, addition of NO donors (300 μM DEA-NONOate) directly induced CaMKII accumulation at excitatory synapses in hippocampal neurons cultured from wildtype (Fig. 5A) but not from CaMKII$^{\Delta SNO}$ mice (Fig. 5B). By contrast, movement to inhibitory synapses was not detected (Fig. 5A and fig. S6A). Notably, NO-induced CaMKII movement was also completely abolished in neurons from mice heterozygous for the CaMKII$^{\Delta SNO}$ mutation (fig. S6B), indicating that nitrosylation of a substantial number of subunits within the 12meric CaMKII holoenzyme is required for the movement to excitatory synapses. Similar to the CaMKII accumulation at excitatory synapses after LTP stimuli, the nitrosylation-induced accumulation was mediated by CaMKII binding to the NMDAR subunit GluN2B, as the GluN2B$^{\Delta CaMKII}$ mutation that prevents CaMKII binding (6, 36) also abolished the synaptic CaMKII accumulation after NO donor application (Fig. 5C). GluN2B binding can also be induced by CaMKII autophosphorylation at Thr^{286} (9, 11), but such autophosphorylation was not required for the NO-induced CaMKII movement, as T286A mutation did not interfere with this movement (Fig. 5D). These results are summarized (Fig. 5E) to provide a direct comparison between the genotypes, showing that the NO-induced CaMKII movement requires CaMKII nitrosylation and binding to GluN2B but not CaMKII autophosphorylation at Thr^{286}. The basal synaptic CaMKII localization without stimulation (measured as spine to dendritic shaft ratio) did not differ between the genotypes (fig. S6C).

CaMKII nitrosylation is not required for acute LTP-induced synaptic accumulation

Synaptic accumulation of CaMKII by GluN2B binding is required in normal LTP (5, 6), and CaMKII nitrosylation directly mediates its corresponding synaptic accumulation in a

Author Manuscript Author Manuscript Author Manuscript Author Manuscript

GluN2B-dependent manner (Fig. 5). Thus, we tested whether the accumulation of CaMKII into excitatory synapses after LTP requires CaMKII nitrosylation. However, accumulation of CaMKII at excitatory synapses that was induced by chemical LTP stimuli (cLTP; 45 sec, 100 μM glutamate, 10 μM glycine) seen in hippocampal neurons from wildtype mice was also observed for the CaMKII$^{\Delta SNO}$ mutant (Fig. 6A,B). At inhibitory synapses, no LTP-induced accumulation was observed for either genotype (Fig. 6C). Thus, CaMKII nitrosylation is not required for the acute, LTP-induced CaMKII movement to excitatory synapses, even though the LTP- and the NO-induced movement are both mediated by GluN2B binding. Notably, this is consistent with electrophysiological observations: Abolishing GluN2B binding impairs HFS-induced LTP (6), but levels of LTP in the CaMKII$^{\Delta SNO}$ mice were normal when induced by HFS and impaired only when induced by TBS (Fig. 4A,B).

Young adult CaMKII$^{\Delta SNO}$ and aged wildtype mice have similarly reduced basal synaptic CaMKII localization

Because nitrosylation did not affect the acute CaMKII movement to synapses in response to LTP stimuli, we decided to test if it may instead chronically affect synapse composition regarding CaMKII content, possibly in a similar way as aging. Thus, we used Western analysis to probe for CaMKII as well as PSD95 and GluN2B in the synaptic PSD fraction and in whole homogenate; we compared protein amount in young-adult wildtype and CaMKII$^{\Delta SNO}$ mice (2 to 3 months old) to aged wildtype mice (18 months old) (Fig. 7). Compared to young adult wildtype mice, both the young adult CaMKII$^{\Delta SNO}$ mice and the aged wildtype mice had significantly less CaMKII in the synaptic fraction (Fig. 7A); by contrast, the amount CaMKII in the total homogenate was the same among the groups (Fig. 7A). For GluN2B, the amount in the total homogenate was reduced only in the aged animal; however, the amount in the synaptic fraction was reduced in aged wildtype and in young adult CaMKII$^{\Delta SNO}$ mice (Fig. 7B). By contrast, the amount of PSD95 was the same among all groups, both in the synaptic fraction and in the total homogenate (Fig. 7C). Thus, synaptic localization of CaMKII appears to be chronically reduced by CaMKII hypo-nitrosylation, which occurs in wildtype mice with aging and in young mice due to the CaMKII$^{\Delta SNO}$ mutation.

Aging decreases hippocampal CaMKII nitrosylation but not oxidation

The decrease in CaMKII nitrosylation with aging that has been described in both mice and humans is currently based on a single study (18). The effect of aging on CaMKII oxidation is unclear, and our CaMKII$^{\Delta SNO}$ mutant prevents both oxidation and nitrosylation of the regulatory domain. Thus, we decided to compare the state of CaMKII nitrosylation and oxidation between hippocampus from young-adult wildtype mice, young adult CaMKII$^{\Delta SNO}$ mice, and aged wildtype mice. For this, we used established biotin-switch methods that detect nitrosylated or oxidized protein by Western analysis of streptavidin pull-down versus total input. Our results indicate that ~12% of CaMKII holoenzymes are nitrosylated in hippocampus from young adult wildtype mice, and that this amount is significantly reduced both in young adult CaMKII$^{\Delta SNO}$ mice and aged wildtype mice (Fig. 8A). By contrast, only minimal levels of CaMKII oxidation were detected, and this did not differ among the ages or genotypes (Fig. 8B). These results further corroborate the notion that CaMKII

Author Manuscript Author Manuscript Author Manuscript Author Manuscript

hypo-nitrosylation can cause the mild impairments in memory and synaptic plasticity that are associated with aging.

DISCUSSION

We showed here that the genetic ablation of CaMKIIα regulation by nitrosylation/oxidation (in the CaMKII$^{\Delta SNO}$ mice) causes impairments both in LTP and in learning and memory that are very similar to the impairments seen in aging. S-nitrosylation was previously shown to generate Ca^{2+}-independent autonomous CaMKII activity (15), and here we showed that it also directly regulates synaptic localization of CaMKII. Notably, though mutations that impair CaMKII localization and generation of autonomy by other mechanisms (pThr^{286} or GluN2B binding) also impair LTP and learning, the specific impairments are very different from the ones associated with aging. Notably, in both aged mice and humans, CaMKII and other neuronal proteins are hypo-nitrosylated (18); by contrast, we did not find any age-related change in CaMKII oxidation. Thus, our findings show that CaMKII hypo-nitrosylation is a plausible cause for the plasticity and learning impairments in aging.

There are multiple mechanisms that can induce Ca^{2+}-independent (autonomous) CaMKII activity, here listed in order of discovery: autophosphorylation at Thr^{286} (8), binding to GluN2B (9), oxidation of Met^{281}/Cys^{289} (14), simultaneous S-nitrosylation of Cys^{280}/Cys^{289} (15), and possibly O-linked-N-acetylglucosaminylation (O-GlcNAcylation) of Ser^{279} (37) (for review see (1, 38). In fact, the discovery that autophosphorylation can generate autonomous activity gave rise to the view of CaMKII as a “memory molecule” (8, 39, 40), long before it was demonstrated that Thr^{286} autophosphorylation indeed plays a crucial role in synaptic plasticity and in learning and memory (4, 13, 41). One thing that all mechanisms for autonomous CaMKII activity have in common is that they all require an initial Ca^{2+}/CaM-stimulus to generate the Ca^{2+}-independent activity (1): Thr^{286} autophosphorylation requires Ca^{2+}/CaM binding in order to expose Thr^{286} as a substrate (42), GluN2B binding requires Ca^{2+}/CaM binding or Thr^{286} autophosphorylation to expose the GluN2B binding site on CaMKII (the T-site) (9), and Ca^{2+}/CaM binding appears to be also required to make Cys^{280}/Cys^{289} accessible for S-nitrosylation (15). Indeed, this initial Ca^{2+} requirement is crucial for these autonomy mechanisms to provide a molecular memory of past Ca^{2+} signals. Notably, these molecular memory mechanisms are not redundant, as individual genetic ablation of each one causes a distinct impairment of LTP and learning and memory. The fact these specific impairments mimic the ones seen aging only after ablation of the S-nitrosylation mechanism is consistent with the fact that aging indeed causes reduced S-nitrosylation of brain protein, including CaMKII.

The hypo-nitrosylation of brain proteins seen in aging is likely caused by age-related overexpression of the S-nitrosoglutathione reductase (GSNOR), an enzyme that limits the amount of bioavailable NO and thereby the level of protein S-nitrosylation. Indeed, experimental overexpression of GSNOR in young mice is sufficient to induce some age-related phenotypes, and GSNOR knockdown in aged mice can alleviate those phenotypes (18). Thus, GSNOR inhibition may be a viable avenue for restoring learning and memory in aging. In either case, our results indicate that restoration of normal CaMKII nitrosylation would be a suitable functional biomarker for any treatment that is designed to improve

Author Manuscript Author Manuscript Author Manuscript Author Manuscript

learning and memory in aging. Because hypo-nitrosylation of CaMKII is sufficient to cause some of the age-related neuronal impairments, reversing this hypo-nitrosylation should be an essential step for improving these impairments.

MATERIALS AND METHODS

Animal and cell culture models

All animal treatment was approved by the University of Colorado Institutional Animal Care and Use Committee, in accordance with NIH guidelines (36). Animals are housed at the Animal Resource Center at the University of Colorado Anschutz Medical Campus (Aurora, CO) and are regularly monitored with respect to general health, cage changes, and overcrowding. Pregnant Sprague-Dawley rats were supplied by Charles River Labs. All mice were bred in-house and cross-bread against C57BL/6 mice. The T286A mice were a generous gift by Ryohei Yasuda, with kind permission by Karl Peter Giese (4, 41). The GluN2B$^{\Delta CaMKII}$ mice were kindly provided by Johannes Hell (6, 36). The CaMKII$^{\Delta SNO}$ mice were made in house, essentially as described for our CaMKIIα knockout line, in which the insertion of a neo-cassette completely silenced gene expression (41). Excision of the neo-cassette allowed expression of the ΔSNO-mutant CaMKII.

Mixed sex wild-type or mutant mouse littermates (on a C57BL/6 background) from heterozygous breeder pairs were used for behavior, slice electrophysiology, or biochemistry. Mixed sex pups from homozygous mice breeder pairs (for CAMKII$^{\Delta SNO}$, CAMKII^{T286A}, GluN2B$^{\Delta CaMKII}$) or mixed sex pups from breeding wild-type with CaMKII$^{\Delta SNO}$ mice (P0-2) or Sprague-Dawley rats (P0) were used to prepare dissociated hippocampal cultures for imaging.

Behavioral tests

Animals were allowed to acclimate to the housing room for two weeks and all animals were handled daily for at least 3 days before starting the behavioral battery. There was an additional 1-hour acclimation period in each testing room before testing. The behavioral tests occurred in order of least to most stressful, with 24 hours between each test as follows: Open Field, Y Maze, Rotarod, Radial Arm Water Maze (RAWM), and finally Contextual Fear Conditioning (CFC). Power analysis using the standard deviations from previous studies (21, 25) indicated that for achieving 80% power with a 30% effect size at an α=0.05 by t-test analysis, the minimum required number of animals were as follows: n=5 for Open Field, n=5 for Y-Maze, n=11 for Rotarod, n=16 for RAWM, and n=11 for CFC (https://clincalc.com/stats/samplesize.aspx). Our main cohort (the young adults; n=22 for wildtype and n=21 for CaMKII$^{\Delta SNO}$ mice) is sufficiently powered for all behavioral tests. By contrast, our additional middle-aged cohort (n=15 for wildtype and n=12 for CaMKII$^{\Delta SNO}$ mice), is not sufficiently powered for the RAWM. Also, although our study used animals from both sexes, it was not sufficiently powered to detect sex differences with confidence. Thus, although we show our results also parsed out by sexes, any results from underpowered analysis are shown only in the supplement, and failure to find statistical significance in these studies does not rule out the possibility of an actual difference.

Author Manuscript Author Manuscript Author Manuscript Author Manuscript

In the open field test, animals were placed into the novel testing chamber and allowed to explore the arena for 20 min. Total distance travelled and time spent in either the center or periphery of the arena was monitored using a video imaging system (EthoVision XT 9).

In the Y-maze test, animals were placed into a Y-shaped maze and allowed to explore for 22 arm entries, or up to 8 min. Each trial was monitored using a video imaging system (EthoVision XT 9) and scored for correct % alternation, where a correct alternation is seen as 3 arm entries without any arm repeats and an incorrect alternation is seen as 3 arm entries with an arm repeat.

In the rotarod test, animals were placed onto a rotating rod, with up to 3 animals tested in a trial, each having their individual lane in the rotarod enclosure. The rotarod apparatus was used in an acceleration mode that gradually increased the speed from 5 to 30 rpm over the course of 5 min. Each animal had 3 trials, at least 5 min apart, where latency to fall off the rod was automatically recorded. Animals that were still on the rod at the end of the 5 min trial were given a score of 300s.

For the radial arm water maze (RAWM) test, a 6 radial-arm maze was placed inside a circular pool that was maintained at 24°C. The testing protocol included two acquisition days that had 10 swim trials each and a testing day with 1 swim trial. On the first acquisition day, the first swim trial included the visible platform, placed into arm 3 (submerged beneath the surface of the water) and all arms except for 3 and 6 were closed off. The animal was then placed into arm 6 and had 1 min to swim to the platform. If the animal failed to reach the platform during this time, it was guided to it. Once on the platform, the animal was allowed to rest there for 30 s, then was returned to its home cage on a heating pad for recovery. Once all animals finished the visible platform trial, the water was then made opaque by adding nontoxic white tempura paint and all arms were opened. Thus, the platform is now hidden for the remaining acquisition days swim trials. For each swim trial, the animal had up to 1 min to find the platform or, if the animal failed to reach the platform during this time, it was guided to it. Animals were allowed to rest on the platform for 30 s before being removed from the maze and returned to its home cage placed on a heating pad allowed to recover for at least 5 min before the next swim trial. The starting arm for each swim trial was pseudo-randomized and latency to reach the platform as well as arm entry order were monitored using a video imaging system (EthoVision XT 9). On the final day of testing, the probe trial, the platform is removed from the maze and the animal is placed into the center of the maze and allowed to explore for 1 min. Arm entry order was again monitored using a video imaging system (EthoVision XT 9). The RAWM was chosen as it combines two individual advantages of two other related tasks: Similar to non-water versions of a radial arm maze, but in contrast to the classic Morris water maze, the RAWM allows additional levels of analysis (including related to working memory). Similar to the classic Morris water maze, but in contrast to non-water versions of a radial arm maze, the RAWM does not require prior food restriction (which is typically required for the non-water versions in order to provide sufficient motivation for the task).

The contextual fear conditioning (CFC) test began with a training day, in which the mice were placed into conditioning box with a metal grid on the floor (MedAssociates). Over a

Author Manuscript Author Manuscript Author Manuscript Author Manuscript

6-min period in the conditioning box, the animals received two separate foot shocks (2 s, 0.7 mA, 2 min interval). The mice were then placed back into their home cage. 24 hours later, on the testing day, the mice were placed into the same box for a 6-min trial without any foot shocks. Movement was measured by a video monitoring system (FreezeScan 2.0) during both days of testing, and freezing behavior was calculated as the percentage of time the mice were immobile.

Mouse hippocampal slice preparation

Hippocampal slices were prepared using 8- to 12-week-old wildtype or CaMKII$^{\Delta SNO}$ mice (except for the LTD-related experiments in the supplement, which used 2-week-old mice instead). Isoflurane anesthetized mice were rapidly decapitated, and the brain was dissected in ice-cold high sucrose solution containing (in mM): 220 sucrose, 12 $MgSO_4$, 10 glucose, 0.2 $CaCl_2$, 0.5 KCl, 0.65 NaH_2PO_4, 13 $NaHCO_3$, and 1.8 ascorbate. Transverse hippocampal slices (400 μm) were made using a tissue chopper (McIlwain) and transferred into 32°C artificial cerebral spinal fluid (ACSF) containing (in mM): 124 NaCl, 3.5 KCl, 1.3 NaH_2 PO4, 26 $NaHCO_3$, 10 glucose, 2 $CaCl_2$, 1 $MgSO_4$, and 1.8 ascorbate. Slices were allowed to recover for at least 1 h. All solutions were saturated with 95% O_2/5% CO_2.

Electrophysiology

All recordings and analysis were performed blind to genotype. A glass micro-pipette was used to record field excitatory post-synaptic potentials (fEPSPs) from the CA1 dendritic layer in response to stimulation in the Schaffer collaterals at the CA2 to CA1 interface using a tungsten bi-polar electrode. Slices were continually perfused with 30.5 ± 0.5°C ACSF at a rate of 3.5 ± 0.5 mL/min during recordings. Stimuli were delivered every 20 sec and 3 responses (1 min) were averaged for analysis. Data were analyzed using WIN LTP with slope calculated as the initial rise from 10 to 60% of response peak. Input/output (I/O) curves were generated by increasing the stimulus intensity at a constant interval until a maximum response or population spike was noted to determine stimulation that elicits 50–70% of maximum slope. Paired-pulse recordings (50 ms inter-pulse interval) were acquired from 50% max slope and no differences in presynaptic facilitation were seen in mutant slices. Stimulus intensity was set to 50% or 70% of the maximum response slope for LTP (TBS, HFS) and LTD (LFS) experiments, respectively. A stable baseline was acquired for a minimum of 20 min prior to TBS (5 episodes of 0.1 Hz, each episode contains 10 stimulus trains of 5 pulses each at 100 Hz), HFS (2 trains of 100 Hz pulses, 20 sec apart), or LFS (900 pulses at 1Hz). For pharmacological inhibition experiments, a stable baseline for a min of 10 min was acquired before treatment with either APV (in DI water) or Nimodipine (in DMSO, final DMSO concentration 0.1%), at which point another 20 min stable baseline was acquired before HFS. The control condition is these experiments was just stimulation application and continuous recording. Change in slope was calculated as a ratio of the average slope of the 20 min baseline. For the HFS experiments, slices from both sexes were used; however, the TBS experiments used only slices from males.

Primary hippocampal culture preparation

To prepare primary hippocampal neurons, hippocampi were dissected from wildtype, CaMKII$^{\Delta SNO}$, CAMKII^{T286A}, or GluN2B$^{\Delta CaMKII}$ mice (P0), incubated in dissociation

Author Manuscript Author Manuscript Author Manuscript Author Manuscript

solution (7 mL HBSS buffered saline, 150 μL 100 mM $CaCl_2$, 10 μL 1 M NaOH, 10 μL 500 mM EDTA, 200 units Papain (Worthington)) for 1 hour, manually dissociated after 5x wash in plating media (MEM, FBS, 50 units/mL pen/strep, 2 mM Glutamax) and plated at 100,000 cells/mL on glass coverslips (poly-D-lysine (0.1mg/mL in 1M Borate Buffer: 3.1g boric acid, 4.75 g borax, in 1 L deionized H20, filter sterilized) and laminin (0.01mg/mL in PBS)-coated 18 mm glass coverslips in 12-well plates). After one day in vitro (DIV 1), media was switched to feeding media (Neurobasal-A, B27 supplements, and 2 mM Glutamax, filter sterilized). At DIV 7, to suppress glial growth, cells were treated with anti-mitotic FDU (70 μM 5-fluoro-2′-deoxyuridine/140 μM uridine), and half of the media was replaced with fresh feeding media. At DIV 12 to 14, neurons were transfected with total cDNA of CaMKII-GFP intrabody, PSD-95-mCherry intrabody, and gephyrin-IRFP intrabody at 1 μg per well using Lipofectamine 2000 (Invitrogen), then treated and imaged 2 to 3 days later.

Image acquisition and analysis

Cells were imaged using a 100 × 1.4NA objective on a Zeiss Axiovert 200 M (Carl Zeiss, Thornwood, NY) controlled by SlideBook software (Intelligent Imaging Innovations, Denver, CO). All imaging analysis was completed using SlideBook software. During image acquisition, neurons were maintained at 34°C. For NO donor experiments, coverslips were imaged in culture media for a 5 min baseline and then treated with either vehicle control (water) or NO donor (DEA-NONOate 300 μM) and imaged for another 10 min, with images collected every minute. For cLTP experiments, coverslips were imaged in ACSF solution (in mM 130 NaCl, 5 KCl, 10 HEPES pH 7.4, 20 glucose, 2 $CaCl_2$, 1 $MgCl_2$, adjusted to proper osmolarity with sucrose. Pre and 1 min post cLTP washout (45 sec cLTP treatment: 100 μM glutamate, 10 μM glycine; 5x fresh ACSF washout) images were collected. 2D maximum intensity projection images were then generated and the mean GFP intensity (CaMKII) at excitatory (PSD-95) or inhibitory (gephyrin) synapses was quantified, as well as the mean intensity of a line drawn in the dendritic shaft. Changes in CaMKII synaptic accumulation were determined by dividing the net change in CaMKII at PSD-95 or gephyrin puncta-to shaft ratio by the pre-stimulation puncta-to-shaft ratio. All representative images were prepared using Fiji software (ImageJ, NIH).

Biotin switch assays of CaMKII S-nitrosylation and oxidation

Biotin switch assay for detection of protein S-nitrosylation was adapted from previous studies (43–45). Previously frozen mouse hippocampi were sonicated in ice cold HENTS buffer (250 mM HEPES pH 7.2. 1 mM EDTA, 0.1 mM neocuprione, 1 % Triton X-100, 0.1 % SDS, 5 mM N-ethylmaleimide, Complete protease inhibitor cocktail (Roche)). Homogenates were centrifuged at 15,000 × g for 10 min at 4°C. Free thiols were blocked by incubating the supernatant in blocking buffer (32 mM N-ethylmaleimide, 2 % SDS, 200 mM HEPES pH 7.2, Complete protease inhibitor cocktail (Roche)) at 50°C for 45 min and vortexing every 3 min. The NEM was removed by acetone precipitating the proteins by addition of two volumes of −20°C acetone, vortexing and incubating at −20°C for 20 min. Proteins were precipitated by centrifugation at 10,000 × g for 10 min at 4°C. The resulting pellet was washed with 700 μl of 70% acetone and centrifuging at 10,000 × g for 5 min at 4°C. The protein pellet was resuspended by sonication in 250 mM HEPES pH 7.2

Author Manuscript Author Manuscript Author Manuscript Author Manuscript

with 1 % SDS. To assess cysteine S-nitrosylation, S-nitrothiols were reduced with 1 mM sodium L-ascorbate and 10 μM cupric sulfate and labeled with 0.25 mM EZ-Link BMCC biotin (ThermoFisher). To assess cysteine oxidation, sulfenic acids were reduced with 20 mM sodium arsenite (46) and labeled with 0.25 mM BMCC-biotin. The reduction/labeling reactions were carried out at room temperature for 1 ½ hours. Unreacted BMCC-biotin was removed from the samples by acetone precipitation as described above. The pellets were resuspended by sonication in 100 μl of 250 mM HEPES pH 7.2 with 1 % SDS, then diluted with 200 μl of neutralization buffer (20 mM HEPES pH 7.7, 1 mM EDTA, 100 mM NaCl, 0.5 % Triton X-100). Protein concentrations were then determined by μl BCA assay (ThermoFisher) and all samples adjusted to 0.3 μg/μl in 300 μl neutralization buffer. For the input, 30 μl of the sample was removed and boiled in Laemmli buffer. Biotinylated proteins were pulled down with 70 μl of a 50% Neutravidin agarose (ThermoFisher) solution in neutralization buffer overnight at 4°C. The unbound supernatant was removed and the Neutravidin agarose was washed three times with 500 μl of high salt wash buffer (20 mM HEPES pH 7.7, 1 mM EDTA, 600 mM NaCl, 0.5 % triton X-100) then twice with regular wash buffer (20 mM HEPES pH 7.7, 1 mM EDTA, 100 mM NaCl). Biotinylated proteins were eluted by boiling for 15 min in 60 μl Laemmli buffer with frequent vortexing. Presence of CaMKIIα was assessed by western blot by loading 7.5 μl (of 40 μl total) of input and 13 μl (of 60 μl total) of pull-downs on 4–20% Criterion gels (Bio-Rad) and blotting as described.

Subcellular Fractionation

Previously frozen hippocampi that had been stored at −80°C were placed in a glass homogenizer containing 1 ml of sucrose homogenization buffer (320 mM sucrose, 10 mM Tris pH 7.4, 1 mM EDTA, 1 mM EGTA, 10 mM NaF, 10 mM NaPPi, 10 mM β-glycerophosphate, 1 μM microcystin LR, and cOmplete protease inhibitor cocktail (Roche)). Hippocampi were homogenized with a teflon pestle (12 passes at 1000 RPM at 4°C). Prior to centrifugation, 45 μl of the total homogenate was removed, sonicated (in 1% SDS, 10 mM Tris pH 7.4, 1 mM EDTA) then boiled at 95°C for 5 min. The remainder of the homogenate was centrifuged at 1,000 × g for 10 min at 4°C. The supernatant was transferred to a fresh tube and then centrifuged at 10,000 × g for 15 min at 4°C. This synaptosomal pellet was then rinsed with sucrose buffer to remove any contaminating supernatant, and then resuspended in 60 μl sucrose buffer. Triton buffer (0.5 % Triton X-100, 10 mM Tris pH 7.4, 1 mM EDTA, 1 mM EGTA, 10 mM NaF, 10 mM NaPPi, 10 mM β-glycerophosphate, 1 μM microcystin LR, and cOmplete protease inhibitor cocktail (Roche)) was then added to the resuspended pellet before homogenization with a hand-held homogenizer. The homogenized pellet was incubated in ice for 30 min, then centrifuged at 32,000 × g for 20 min at 4°C to produce a PSD-enriched pellet. This PSD-enriched fraction was then sonicated (in 1% SDS, 10 mM Tris pH 7.4, 1 mM EDTA) and then boiled at 95°C for 5 min. Total protein concentration of the homogenate and PSD-fraction were determined by BCA protein assay kit (Pierce).

CaMKII activity assays in HEK cell extracts

Wildtype and nitrosylation/oxidation deficient mutant ($CaMKII^{\Delta SNO}$) of CaMKIIα were transfected into HEK-293 cells (a commonly used human cell line) by Calcium phosphate

Author Manuscript Author Manuscript Author Manuscript Author Manuscript

precipitation. After three days CaMKII was solubilized. Briefly, cells were homogenized with a motorized pellet pestle (Kontes) for 10 sec in 0.4 ml ice cold 50 mM PIPES pH 7.2, 10% glycerol, 1 mM EDTA, 1 mM DTT and complete protease inhibitor (Roche), then centrifuged at 16,000 × g for 20 min. The CaMKII concentration from the resulting supernatant was determined by western blot using purified recombinant CaMKIIα as a standard. CaMKII activity assays: Ca^{2+}/calmodulin-stimulated activity and autonomous activity after Thr^{286} autophosphorylation was assessed by ^{32}P incorporation into the peptide substrate syntide 2, either in presence of Ca^{2+}/CaM (1.2 mM/1 μM) or EGTA (1.5 mM), as previously described (15, 35). Prior to activity assays, HEK cell extracts containing CaMKIIα were adjusted to contain 100 nM CaMKIIα and equal total protein concentrations. CaMKIIα was selectively autophosphorylated at Thr^{286} by reacting with 1.5 CaCl2, 1 CaM, 10 MgCl2, 0.1 ATP, 1 μM Microcystin LR, 50 PIPES pH 7.2 in ice for 10 min. The autophosphorylation reaction was stopped by diluting 8-fold with addition of 5 EDTA.

Western blotting and analysis

Before undergoing SDS-PAGE, samples were boiled in Laemmli sample buffer for 5 min at 95° C. Proteins were separated in a resolving phase polymerized from 10% acrylamide, then transferred to a polyvinylidene difluoride membrane at 24 V for 1 hour at 4° C. Membranes were blocked in 5% milk and incubated with mouse anti-CaMKII (1:2000; BD Biosciences, RRID: AB_398819), mouse anti PSD-95 (1:2500; NeuroMab, RRID: AB_10698024) or mouse anti-GluN2B (1:1000; Cell Signaling Technology, RRID: AB_2798506) followed by incubation with HRP-linked anti-mouse IgG (1:6000; GE Healthcare, RRID: AB_772210). Blots were developed using chemiluminescence (Super Signal West Femto, Thermo-Fisher), imaged using the Chemi-Imager 4400 system (Alpha-Innotech), and analyzed by densitometry (Alphaese FC).

Quantification and statistical analysis

All data are shown as mean ± SEM. Statistical significance is indicated in the figure legends. Imaging experiments were obtained and analyzed using SlideBook 6.0 software. Western blots were analyzed using ImageJ (NIH). The remaining statistical analyses were performed using Prism (GraphPad 9.5.0) software. Tests are two-sided with alpha set at 0.05. All data were tested for their ability to meet parametric test assumptions by plotting data distributions and calculating variances. Both the t-test and the ANOVA are robust for use in small sample sizes (<20) as long as the data have similar distributions and sample sizes. For data with obvious skew or outliers or different variances, non-parametric tests were used. For sample sizes >20, the data were further evaluated by a Shapiro-Wilk test for normal distribution and a Brown-Forsythe test (3 or more groups) or an F-test (2 groups) to determine equal variance. If the data failed these tests, the non-parametric equivalent test was used. Two independent samples were analyzed using unpaired, two-tailed Student’s t-tests or the Mann-Whitney U test. Comparisons between three or more groups were done by one-way ANOVA (or the non-parametric Kruskal-Wallis test) with specific post-hoc analysis indicated in figure legends. Comparisons between three or more groups with two independent variables were assessed by two-way ANOVA with Bonferroni post-hoc test to determine whether there is an interaction and/or main effect between the variables, unless

Author Manuscript Author Manuscript Author Manuscript Author Manuscript

otherwise stated. The definition of “n” in our experiments as follows: animal number in behavioral testing, slice number in electrophysiological recordings (from at least 3 different animals), neurons in imaging experiments (from at least 3 different cultures), and samples for biochemistry (each collected from different animals).

Supplementary Material

Refer to Web version on PubMed Central for supplementary material.

Acknowledgements:

We thank Janna Mize-Berge for help with mouse colony maintenance. We thank Dr. Kathleen Torkko for advice regarding statistical analysis.

Funding:

This work was supported by National Institutes of Health grants T32 AG000279 (supporting N.L.R.), F31 AG069458 (to N.L.R.), R01 NS040701 and R01 MH123700 (to M.L.D.), R01 NS081248, R01 NS118786, and R01 AG067713 (to K.U.B.).

Data and materials availability:

All reasonable material requests will be fulfilled and should be addressed to the corresponding author. All data needed to evaluate the conclusions are present in the paper. Additionally, the datasets generated during this study are available through Mendeley (doi: 10.17632/2chhct47wx.1).

REFERENCES AND NOTES

1. Bayer KU, Schulman H, CaM Kinase: Still Inspiring at 40. Neuron 103, 380–394 (2019). [PubMed: 31394063]
2. Lisman J, Yasuda R, Raghavachari S, Mechanisms of CaMKII action in long-term potentiation. Nature reviews. Neuroscience 13, 169–182 (2012). [PubMed: 22334212]
3. Hell JW, CaMKII: claiming center stage in postsynaptic function and organization. Neuron 81, 249–265 (2014). [PubMed: 24462093]
4. Giese KP, Fedorov NB, Filipkowski RK, Silva AJ, Autophosphorylation at Thr286 of the alpha calcium-calmodulin kinase II in LTP and learning. Science 279, 870–873 (1998). [PubMed: 9452388]
5. Barria A, Malinow R, NMDA receptor subunit composition controls synaptic plasticity by regulating binding to CaMKII. Neuron 48, 289–301 (2005). [PubMed: 16242409]
6. Halt AR et al. , CaMKII binding to GluN2B is critical during memory consolidation. EMBO J. 31, 1203–1216 (2012). [PubMed: 22234183]
7. Larsen ME, Buonarati OR, Qian H, Hell JW, Bayer KU, Stimulating beta-adrenergic receptors promotes synaptic potentiation by switching CaMKII movement from LTD to LTP mode. J Biol Chem 299, 104706 (2023). [PubMed: 37061000]
8. Miller SG, Kennedy MB, Regulation of brain type II Ca2+/calmodulin-dependent protein kinase by autophosphorylation: a Ca2+-triggered molecular switch. Cell 44, 861–870 (1986). [PubMed: 3006921]
9. Bayer KU, De Koninck P, Leonard AS, Hell JW, Schulman H, Interaction with the NMDA receptor locks CaMKII in an active conformation. Nature 411, 801–805 (2001). [PubMed: 11459059]
10. Lisman JE, McIntyre CC, Synaptic plasticity: a molecular memory switch. Curr Biol 11, R788–791 (2001). [PubMed: 11591339]

Author Manuscript Author Manuscript Author Manuscript Author Manuscript

11. Strack S, McNeill RB, Colbran RJ, Mechanism and regulation of calcium/calmodulin-dependent protein kinase II targeting to the NR2B subunit of the N-methyl-D-aspartate receptor. J Biol Chem 275, 23798–23806 (2000). [PubMed: 10764765]
12. O'Leary H, Liu WH, Rorabaugh JM, Coultrap SJ, Bayer KU, Nucleotides and phosphorylation bi-directionally modulate Ca2+/calmodulin-dependent protein kinase II (CaMKII) binding to the N-methyl-D-aspartate (NMDA) receptor subunit GluN2B. J Biol Chem 286, 31272–31281 (2011). [PubMed: 21768120]
13. Cook SG, Rumian NL, Bayer KU, CaMKII T286 phosphorylation has distinct essential functions in three forms of long-term plasticity. J Biol Chem, 102299 (2022).
14. Erickson JR et al. , A dynamic pathway for calcium-independent activation of CaMKII by methionine oxidation. Cell 133, 462–474 (2008). [PubMed: 18455987]
15. Coultrap SJ, Bayer KU, Nitric oxide induces Ca2+-independent activity of the Ca2+/calmodulin-dependent protein kinase II (CaMKII). J Biol Chem 289, 19458–19465 (2014). [PubMed: 24855644]
16. Sen N, Snyder SH, Protein modifications involved in neurotransmitter and gasotransmitter signaling. Trends Neurosci 33, 493–502 (2010). [PubMed: 20843563]
17. Nakamura T et al. , Aberrant protein s-nitrosylation in neurodegenerative diseases. Neuron 78, 596–614 (2013). [PubMed: 23719160]
18. Zhang Y et al. , Increased GSNOR Expression during Aging Impairs Cognitive Function and Decreases S-Nitrosation of CaMKIIalpha. J Neurosci 37, 9741–9758 (2017). [PubMed: 28883020]
19. Blank T, Nijholt I, Kye MJ, Radulovic J, Spiess J, Small-conductance, Ca2+-activated K+ channel SK3 generates age-related memory and LTP deficits. Nat Neurosci 6, 911–912 (2003). [PubMed: 12883553]
20. Foster TC, Dissecting the age-related decline on spatial learning and memory tasks in rodent models: N-methyl-D-aspartate receptors and voltage-dependent Ca2+ channels in senescent synaptic plasticity. Prog Neurobiol 96, 283–303 (2012). [PubMed: 22307057]
21. Lamberty Y, Gower AJ, Age-related changes in spontaneous behavior and learning in NMRI mice from maturity to middle age. Physiology & behavior 47, 1137–1144 (1990). [PubMed: 2395918]
22. Shukitt-Hale B, McEwen JJ, Szprengiel A, Joseph JA, Effect of age on the radial arm water maze-a test of spatial learning and memory. Neurobiology of aging 25, 223–229 (2004). [PubMed: 14749140]
23. Gorina YV et al. , [The battery of tests for behavioral phenotyping of aging animals in the experiment]. Advances in gerontology = Uspekhi gerontologii 30, 49–55 (2017). [PubMed: 28557390]
24. Shoji H, Takao K, Hattori S, Miyakawa T, Age-related changes in behavior in C57BL/6J mice from young adulthood to middle age. Molecular brain 9, 11 (2016). [PubMed: 26822304]
25. Shoji H, Miyakawa T, Age-related behavioral changes from young to old age in male mice of a C57BL/6J strain maintained under a genetic stability program. Neuropsychopharmacol Rep 39, 100–118 (2019). [PubMed: 30816023]
26. Gage FH, Dunnett SB, Bjorklund A, Spatial learning and motor deficits in aged rats. Neurobiology of aging 5, 43–48 (1984). [PubMed: 6738785]
27. Magnusson KR et al. , Age-related deficits in mice performing working memory tasks in a water maze. Behavioral neuroscience 117, 485–495 (2003). [PubMed: 12802877]
28. Dudek SM, Bear MF, Bidirectional long-term modification of synaptic effectiveness in the adult and immature hippocampus. J Neurosci 13, 2910–2918 (1993). [PubMed: 8331379]
29. Norris CM, Halpain S, Foster TC, Reversal of age-related alterations in synaptic plasticity by blockade of L-type Ca2+ channels. J Neurosci 18, 3171–3179 (1998). [PubMed: 9547225]
30. Veng LM, Mesches MH, Browning MD, Age-related working memory impairment is correlated with increases in the L-type calcium channel protein alpha1D (Cav1.3) in area CA1 of the hippocampus and both are ameliorated by chronic nimodipine treatment. Brain research. Molecular brain research 110, 193–202 (2003). [PubMed: 12591156]
31. Shankar S, Teyler TJ, Robbins N, Aging differentially alters forms of long-term potentiation in rat hippocampal area CA1. J Neurophysiol 79, 334–341 (1998). [PubMed: 9425202]

Author Manuscript Author Manuscript Author Manuscript Author Manuscript

32. Boric K, Munoz P, Gallagher M, Kirkwood A, Potential adaptive function for altered long-term potentiation mechanisms in aging hippocampus. J Neurosci 28, 8034–8039 (2008). [PubMed: 18685028]
33. Robillard JM, Gordon GR, Choi HB, Christie BR, MacVicar BA, Glutathione restores the mechanism of synaptic plasticity in aged mice to that of the adult. PLoS One 6, e20676 (2011). [PubMed: 21655192]
34. Cook SG, Goodell DJ, Restrepo S, Arnold DB, Bayer KU, Simultaneous live-imaging of multiple endogenous proteins reveals a mechanism for Alzheimer's-related plasticity impairment. Cell Rep 27, 658–665 (2019). [PubMed: 30995464]
35. Cook SG, Buonarati OR, Coultrap SJ, Bayer KU, CaMKII holoenzyme mechanisms that govern the LTP versus LTD decision. Sci Adv 7, (2021).
36. Buonarati OR et al. , CaMKII versus DAPK1 binding to GluN2B in ischemic neuronal cell death after resuscitation from cardiac arrest. Cell Rep 30, 1–8 (2020). [PubMed: 31914378]
37. Erickson JR et al. , Diabetic hyperglycaemia activates CaMKII and arrhythmias by O-linked glycosylation. Nature 502, 372–376 (2013). [PubMed: 24077098]
38. Coultrap SJ, Bayer KU, CaMKII regulation in information processing and storage. Trends Neurosci 35, 607–618 (2012). [PubMed: 22717267]
39. Lisman JE, A mechanism for memory storage insensitive to molecular turnover: a bistable autophosphorylating kinase. Proc Natl Acad Sci U S A 82, 3055–3057 (1985). [PubMed: 2986148]
40. Lisman JE, Goldring MA, Feasibility of long-term storage of graded information by the Ca2+/calmodulin-dependent protein kinase molecules of the postsynaptic density. Proc Natl Acad Sci U S A 85, 5320–5324 (1988). [PubMed: 3393540]
41. Coultrap SJ et al. , Autonomous CaMKII mediates both LTP and LTD using a mechanism for differential substrate site selection. Cell Reports 6, 431–437 (2014). [PubMed: 24485660]
42. Hanson PI, Meyer T, Stryer L, Schulman H, Dual role of calmodulin in autophosphorylation of multifunctional CaM kinase may underlie decoding of calcium signals. Neuron 12, 943–956 (1994). [PubMed: 8185953]
43. Jaffrey SR, Snyder SH, The biotin switch method for the detection of S-nitrosylated proteins. Sci STKE 2001, pl1 (2001).
44. Kettenhofen NJ, Wang X, Gladwin MT, Hogg N, In-gel detection of S-nitrosated proteins using fluorescence methods. Methods Enzymol 441, 53–71 (2008). [PubMed: 18554529]
45. Wang X, Kettenhofen NJ, Shiva S, Hogg N, Gladwin MT, Copper dependence of the biotin switch assay: modified assay for measuring cellular and blood nitrosated proteins. Free Radic Biol Med 44, 1362–1372 (2008). [PubMed: 18211831]
46. Saurin AT, Neubert H, Brennan JP, Eaton P, Widespread sulfenic acid formation in tissues in response to hydrogen peroxide. Proc Natl Acad Sci U S A 101, 17982–17987 (2004). [PubMed: 15604151]

Author Manuscript Author Manuscript Author Manuscript Author Manuscript

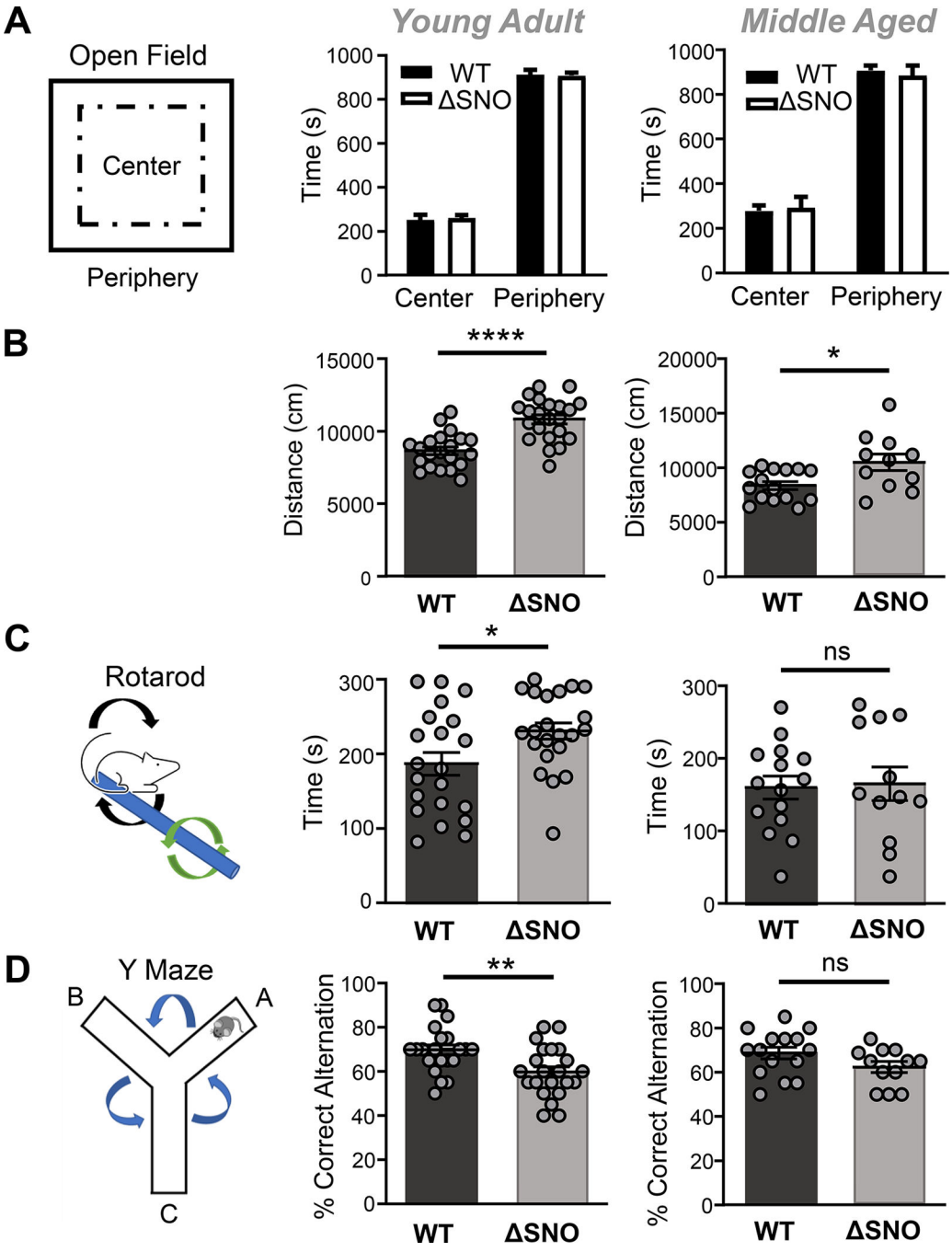

Figure 1: The CaMKII$^{\Delta SNO}$ mice have mild impairments in working memory but not in locomotor coordination.

(A to D) Behavior tests in young-adult and middle-aged wild-type and CaMKII$^{\Delta SNO}$ mice, showing the amount of time spent in the center and periphery of the testing chamber in the Open Field test (A), the distance travelled in the Open Field test (B), the time spent on the rod in the Rotarod test (C), and the percent correct alternation in the Y-Maze test (D). Error bars indicate SEM; n=21 young adult wild-type, 22 young adult CaMKII$^{\Delta SNO}$, 15 middle aged wild-type, and 12 middle aged CaMKII$^{\Delta SNO}$ mice. $^{ns}p>0.05$, *p<0.05 (0.012 in B, 0.023 in C), **p<0.01 (0.005 in D), and ****p<0.0001 by unpaired t-test.

Author Manuscript Author Manuscript Author Manuscript Author Manuscript

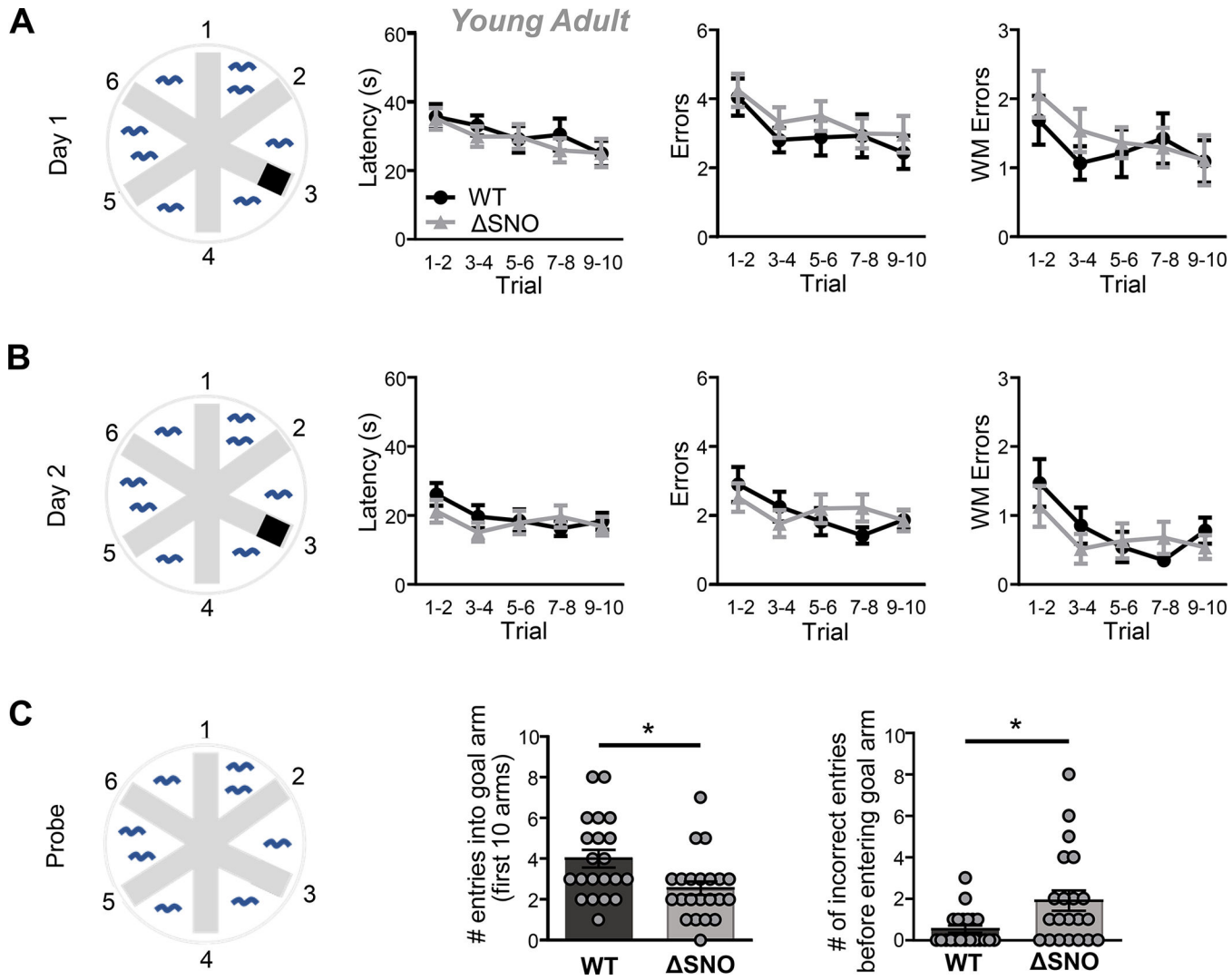

Figure 2: The CaMKII$^{\Delta SNO}$ mice have mild long-term memory impairments in the RAWM.

(A to C) Testing of young adult wild-type and young adult CaMKII$^{\Delta SNO}$ mice in the Radial Arm Water Maze (RAWM), assessing latency, errors, and working memory errors in reaching the platform on training day 1 (A) and training day 2 (B), and the number of entries into the goal arm during the probe trial (C). Error bars indicate SEM; n=21 young adult wild-type and 22 young adult CaMKII$^{\Delta SNO}$ mice. $^{ns}p>0.05$, *$p<0.05$ (0.012) by unpaired t-test.

Author Manuscript Author Manuscript Author Manuscript Author Manuscript

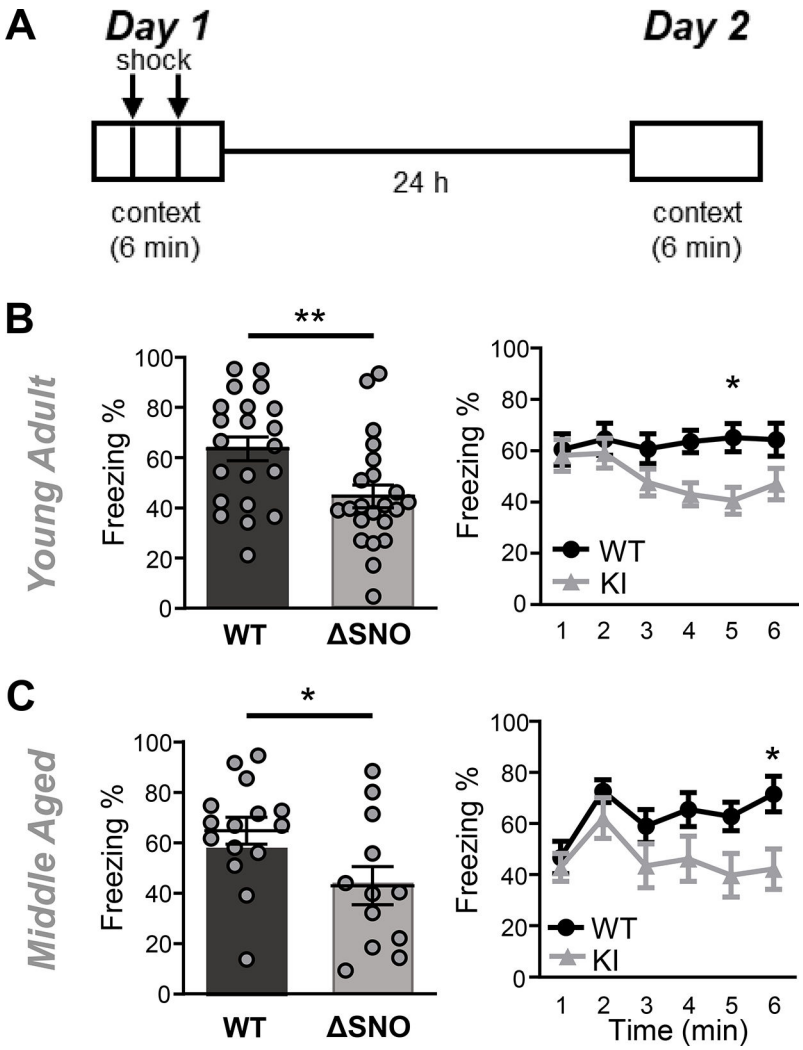

Figure 3: The CaMKII$^{\Delta SNO}$ mice have mild long-term memory impairments in contextual fear conditioning.

(A) Schematic and timeline of the Contextual Fear Conditioning (CFC) task. **(B and C)** Percent freezing observed in the young-adult (B) and middle-aged (C) wild-type and CaMKII$^{\Delta SNO}$ mice in the CFC test, during the last 4 min of testing [left; **p≤0.01 (0.007 in B, 0.0226 in C) by unpaired t-test] and over the full time-course (right; *p<0.05 at the marked time point, by two-way ANOVA with Bonferroni post hoc test). Error bars indicate SEM; n=21 wild-type and 22 CaMKII$^{\Delta SNO}$ mice in each age group.

Author Manuscript Author Manuscript Author Manuscript Author Manuscript

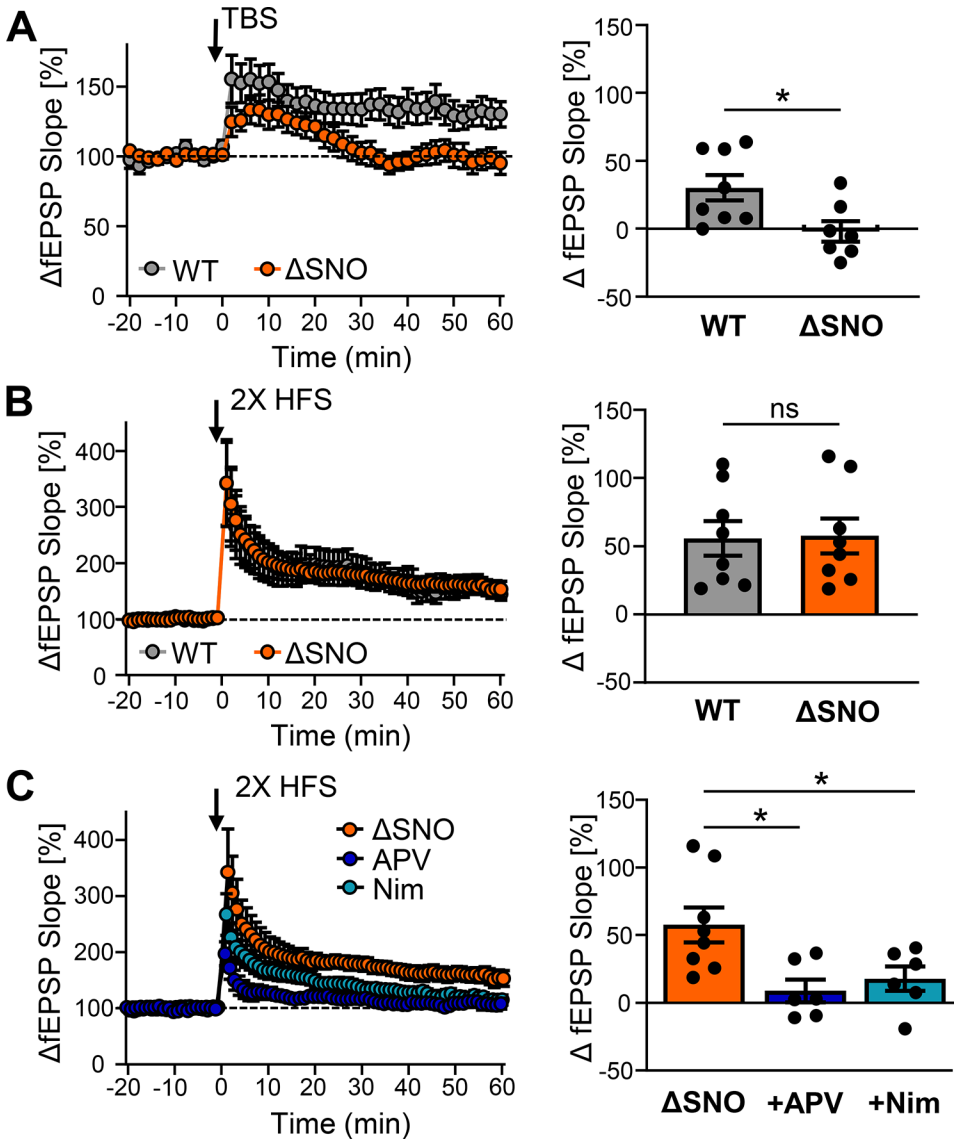

Figure 4: The mild LTP impairments in CaMKII$^{\Delta SNO}$ mice are similar as previously described for aged mice.

(A) The change in fEPSP slope for TBS-induced LTP in hippocampal slices from wild-type and CaMKII$^{\Delta SNO}$ mice. n=8 wild-type and 9 CaMKII$^{\Delta SNO}$ slices from at least 5 different animals. *p<0.05 (0.022) by unpaired t-test. **(B)** The change in fEPSP slope for HFS-induced LTP in wild-type and CaMKII$^{\Delta SNO}$ mice. n=8 hippocampal slices from at least 7 animals, per group; ^{ns}p>0.05. **(C)** The change in fEPSP slope for HFS-induced LTP in CaMKII$^{\Delta SNO}$ mice, when additionally treated with 10 μM APV or 10 μM nimodipine. n=8 control slices and 6 APV- or nimodipine-treated slices, from at least 4 different animals per group. Data for ΔSNO control (orange) is the same as in panel B. *p<0.05 (0.012 for APV; 0.04 for nimodipine) by one-way ANOVA with Bonferroni post hoc versus ΔSNO. In all panels, error bars indicate SEM.

Author Manuscript Author Manuscript Author Manuscript Author Manuscript

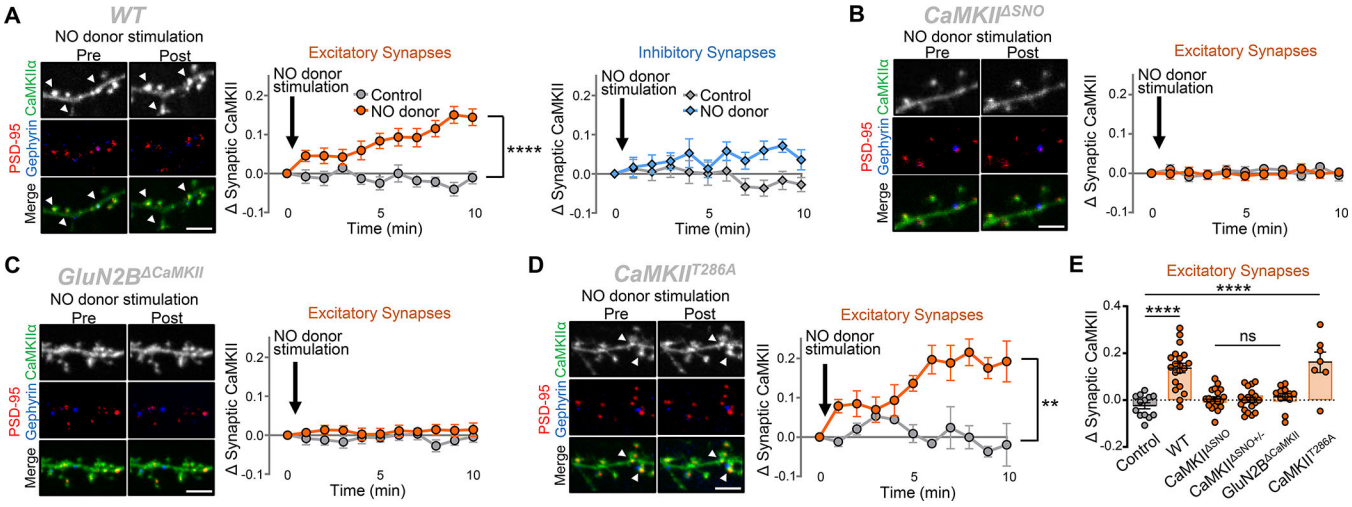

Figure 5: NO induces CaMKII movement to synapses mediated by GluN2B binding.

(A) In neurons cultured from wild-type mice, CaMKII accumulation into excitatory or inhibitory synapses after treatment with NO donor (300 μM DEA-NONOate) or vehicle (water; Control), applied at the timepoint indicated by the arrows and remained on the hippocampal cultures throughout the imaging. Error bars indicate SEM; n=13 control and 20 NO donor-treated wild-type neurons from at least 3 different cultures. ****p<0.0001 by two-way ANOVA with Bonferroni post hoc test. Scale bar, 5 μM. **(B)** In neurons cultured from CaMKII$^{\Delta SNO}$ mice, CaMKII accumulation to excitatory synapses after treatment as in (A). Error bars indicate SEM; n=22 control and 19 NO donor-treated neurons from at least 3 different cultures. p>0.05 by two-way ANOVA with Bonferroni post hoc test. Scale bar, 5 μM. **(C)** As in (B), in neurons cultured from GluN2B$^{\Delta CaMKII}$ mice. n=11 control and 12 NO donor-treated neurons from at least 3 different cultures. p>0.05. **(D)** As in (B), in neurons cultured from CaMKII^{T286A} mice. n=3 control and 7 NO donor-treated neurons from at least 3 different cultures. **p<0.01. **(E)** Comparison graph of CaMKII accumulation to excitatory synapses after NO donor stimulation in the various genotypes from (A to D). Error bars and n as stated above. ****p<0.0001 versus control by one-way ANOVA with Bonferroni post hoc test.

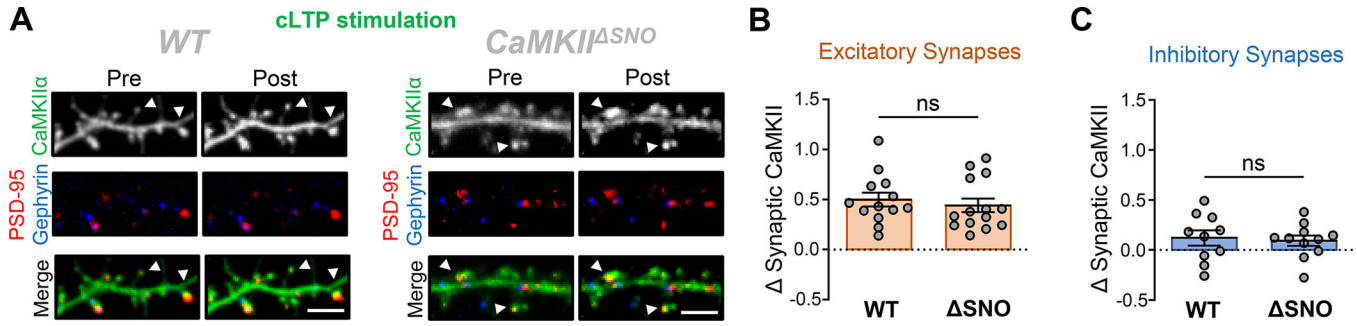

Figure 6: CaMKII nitrosylation is not required for acute LTP-induced CaMKII movement.

(A) Representative images of cultured neurons from wild-type and CaMKII$^{\Delta SNO}$ mice before (pre) and after (post) cLTP stimulation. Error bars indicate SEM; n= 13 wild-type and 14 CaMKII$^{\Delta SNO}$ neurons. Scale bars, 5 μM. **(B and C)** CaMKII accumulation to excitatory (B) and inhibitory (C) synapses after cLTP stimulation in wild-type and CaMKII$^{\Delta SNO}$ neurons. Error bars indicate SEM; n= respectively 13 and 10 wild-type and 14 and 11 CaMKII$^{\Delta SNO}$ neurons, each group from at least 3 different cultures. $^{ns}p>0.05$ by unpaired t-test.

Author Manuscript Author Manuscript Author Manuscript Author Manuscript

Author Manuscript Author Manuscript Author Manuscript Author Manuscript

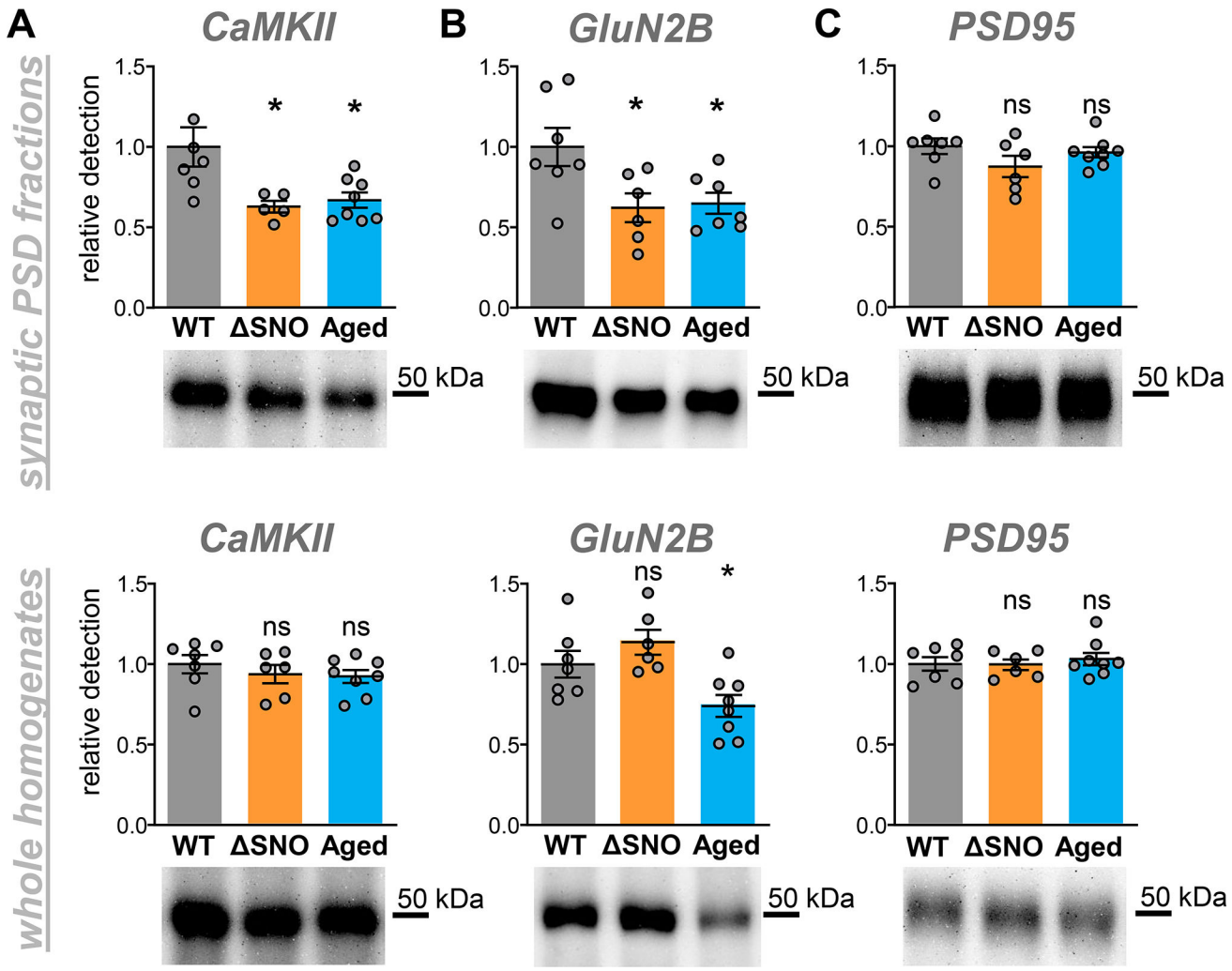

Figure 7: Young adult CaMKII$^{\Delta SNO}$ mice show similarly reduced synaptic CaMKII levels as aged wildtype mice.

(A to C) Western blotting analysis for the amount of (A) CaMKII, (B) GluN2B, and (C) PSD95 in synaptic PSD fractions (top) and total homogenates (bottom) from hippocampal tissues of young adult wild-type mice, young adult CaMKII$^{\Delta SNO}$ mice, and aged wild-type mice. Error bars indicate SEM; n=6 or 7 young adult wild-type, 6 young adult CaMKII$^{\Delta SNO}$, and 8 aged wild-type animals. $^{ns}p>0.05$, *$p<0.05$ by one-way ANOVA with Neuman-Keuls post hoc test.

Author Manuscript Author Manuscript Author Manuscript Author Manuscript

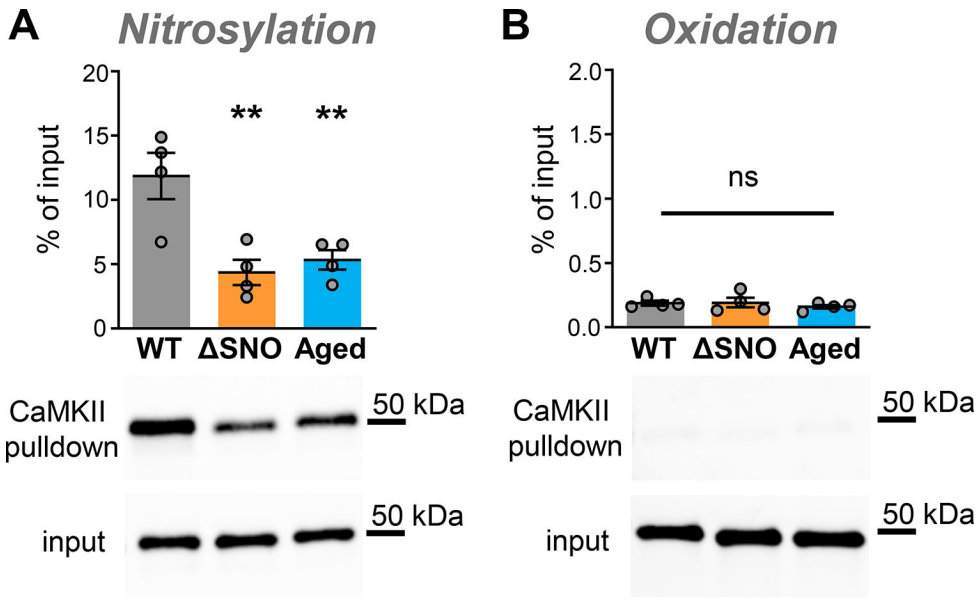

Figure 8: Young adult CaMKII$^{\Delta SNO}$ mice show similarly reduced nitrosylation levels as aged wildtype mice.

(A and B) Biotin switch assay for detection of (A) nitrosylation or (B) oxidation levels in homogenized hippocampi from young adult wild-type mice, young adult CaMKII$^{\Delta SNO}$ and aged wild-type mice and compared by Western blotting analysis. Error bars indicate SEM in all panels, from n=4 mice per age/genotype group. **p<0.01 by one-way ANOVA with Neuman-Keuls post hoc test.

Author Manuscript Author Manuscript Author Manuscript Author Manuscript

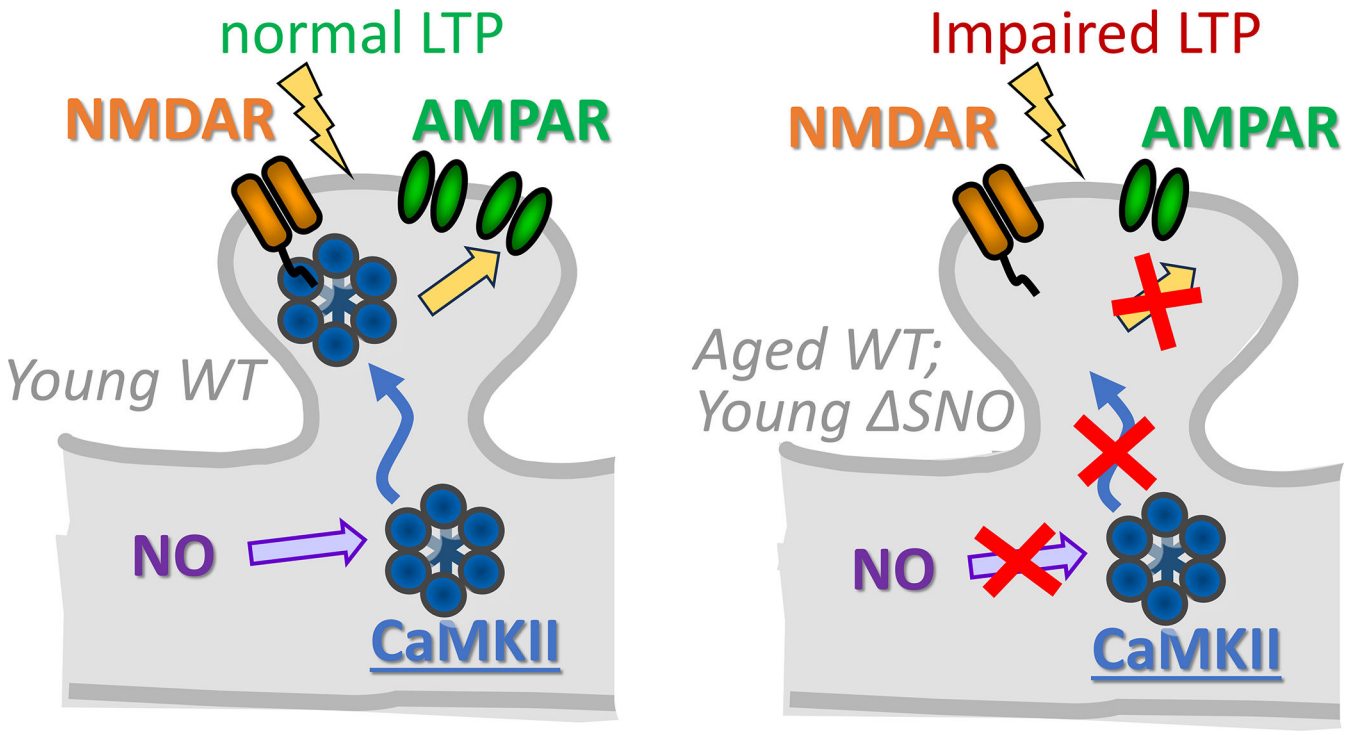

Figure 9: Model of the mechanism.

The illustrations depict dendritic spines, which form the postsynaptic side of excitatory synapses, featuring CaMKII (blue), the NMDA-type glutamate receptor (NMDAR; burnt orange) and the AMPA-type glutamate receptor (AMPAR; green). Nitric oxide (NO; purple) can induce S-nitrosylation of the CaMKII regulatory domain at $Cys^{280/289}$, which directly causes CaMKII accumulation at excitatory synapses through direct binding to the NMDAR subunit GluN2B (left panel). Whereas S-nitrosylation is not required for the similar accumulation in response to LTP-stimuli, a reduction of this S-nitrosylation (either by reduced NO during aging or by genetic mutation) causes a chronic reduction of CaMKII at synapses (right panel). Notably, the ΔSNO mutation that prevents CaMKII S-nitrosylation at $Cys^{280/289}$ caused similar memory and LTP impairments (illustrated by impaired regulation of AMPARs) in the young-adult mutant mice as previously demonstrated in aged wild-type mice. Whereas the level of potentiation was reduced only for TBS-induced LTP, the apparently normal level of potentiation of HFS-induced LTP required not only stimulation NMDARs (as in young-adult, wild-type mice) but also L-type voltage gated Ca^{2+}-channels.